ACS OMEGA

http://pubs.acs.org/journal/acsodf

Article

Understanding the Contribution of Individual Amino Acid Residues in the Binding of Psychoactive Substances to Monoamine Transporters

Tamara Senior, Michelle J. Botha, Alan R. Kennedy, and Jesus Calvo-Castro*

Cite This: https://dx.doi.org/10.1021/acsomega.0c01370

Read Online

ACCESS | Metrics & More | Article Recommendations | Supporting Information

ABSTRACT: The development of point-of-care detection methodologies for biologically relevant analytes that can facilitate rapid and appropriate treatment is at the forefront of current research efforts and interests. Among the various approaches, those exploiting host−guest chemistries where the optoelectronic signals of the chemical sensor can be modulated upon interaction with the target analyte are of particular interest. In aiding their rational development, judicious selection of peripheral functional groups anchored to core motifs with desired properties is critical. Herein, we report an in-depth investigation of the binding of three psychoactive substances, MDAI, mexedrone, and phenibut, to receptors of the monoamine transporters for dopamine, norepinephrine, and serotonin, particularly focusing on the role of individual amino acid residues. We first evaluated the conformational flexibility of the ligands by comparing their experimentally determined crystal structure geometries to those optimized by means of quantum as well as molecular mechanics, observing significant changes in the case of phenibut. Molecular docking studies were employed to identify preferential binding sites by means of calculated docking scores. In all cases, irrespective of the monoamine transporter, psychoactive substances exhibited preferred interaction with the S1 or central site of the proteins, in line with previous studies. However, we observed that experimental trends for their relative potency on the three transporters were only reproduced in the case of mexedrone. Subsequently, to further understand these findings and to pave the way for the rational development of superior chemical sensors for these substances, we computed the individual contributions of each nearest neighbor amino acid residue to the binding to the target analytes. Interestingly, these results are now in agreement with those experimental potency trends. In addition, these observations were in all cases associated with key intermolecular interactions with neighboring residues, such as tyrosine and aspartic acid, in the binding of the ligands to the monoamine transporter for dopamine. As a result, we believe this work will be of interest to those engaged in the rational development of chemical sensors for small molecule analytes as well as to those interested in the use of computational approaches to further understand protein−ligand interactions.

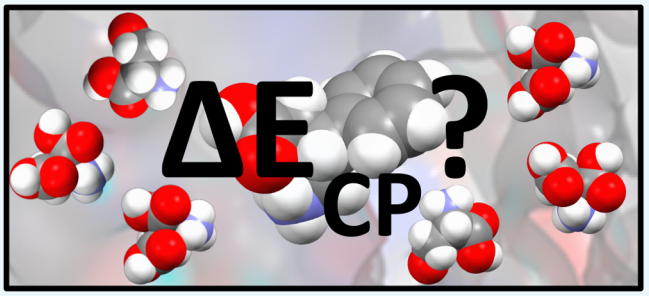

INTRODUCTION

Among the plethora of chemicals that regulate normal brain function, monoamine transporters (MATs) are widely considered to play a critically important role.[1,2] Located in the plasma membranes of the monoaminergic neurons, they consist of 12 transmembrane helices and are responsible for the release or reuptake of the monoamines dopamine, norepinephrine, and serotonin, which have biological roles spanning from mood stabilization and appetite to sexual arousal and decision making.[3−7]

Dopamine concentrations in the brain, which are modulated by the dopamine transporter (DAT), can be further modified by ligands that interact with the protein by either inhibiting the reuptake of dopamine and leading to feelings of euphoria or by stimulating the release of synaptic dopamine (i.e., amphetamine), associated with increased confidence and levels of energy.[4,8,9] In turn, the serotonin monoamine transporter (SERT) is responsible for maintaining normal concentrations of serotonin in the brain, with unregulated concentrations resulting in a number of disorders such as anxiety, depression, and impaired cognitive function.[10,11] In relation to the norepinephrine transporter (NET), which recycles the three monoamines from the synapse to the presynaptic neurons, there exist a smaller number of selective ligands that have been identified to date in comparison to ligands that are selective toward the other two monoamine transporters, which can be accounted for on the basis of the structural similarity between

Received: March 26, 2020
Accepted: June 19, 2020

the DAT and the NET.[12−15] The latter can be further ascribed to the large structural similarities among the three monoamines, particularly in the cases of dopamine and norepinephrine (Figure 1), leading to a degree of promiscuity

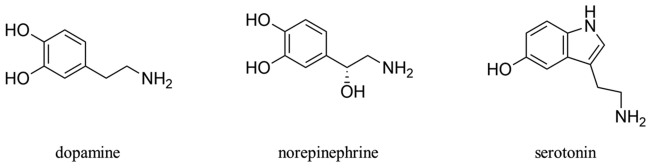

Figure 1. Chemical structures for dopamine, norepinephrine, and serotonin.

between them and their associated transporters and furthermore to the development of drugs that exhibit affinities to all three monoamine transporters.[3,7,12,16,17] Along those lines and associated with the extensive roles in cognitive and emotional processes played by monoamine transporters, drug substances such as cocaine, amphetamine, and ecstasy, which are structurally related to the monoamines, have been extensively utilized recreationally to alter the monoamine transporter levels within the brain to elicit some form of psychoactive response.[18−20] More recently, the so-called novel psychoactive substances (NPSs), which denote compounds that intend to imitate the psychoactive effects of other controlled ones in an attempt to bypass existing regulations, have emerged in the illegal markets for recreational substances.[21,22] Primarily due to their associated fast rate of appearance and their low residence time in these markets, there is an acknowledged lack of easily accessible detection and identification platforms for NPSs that prevent rapid and appropriate treatment. The latter further makes them a critical social and health problem of worldwide concern.[23] Considering these characteristics of NPSs, the development of point-of-care detection methodologies for NPSs is at the forefront of research interests and efforts.[24]

Drugs, recreational or therapeutic, act on target receptors via appropriate supramolecular interactions to either trigger or block biological responses. That concept, widely exploited by pharmacophore modeling approaches in ligand-based drug development methodologies,[25−27] has also been utilized in the rational development of chemical sensors.[28] These methodologies exploit host−guest type chemistries whereby the interaction leads to measurable changes in the optoelectronic properties of the host, hence facilitating the detection of the target analyte. As a result, in-depth understanding of the intermolecular interactions that would foster selective binding between the chemical sensor (host) and the target analyte (guest) is deemed critical in the development of novel sensing platforms for biologically relevant analytes, such as psychoactive substances. In most cases, those interactions are noncovalent in nature, which although individually weak, play a critical role in defining the overall binding affinities and associate conformational changes in a plethora of key processes that are not limited to protein-binding interactions and drug development but that further span to other topical areas of research such as charge-transfer mechanisms in optoelectronic materials.[29−34]

Along those lines, understanding any structural causation upon interaction between ligands and receptors would be invaluable in aiding the development of selective chemical sensors for their target analytes, by guiding the selection of peripheral substitutions performed on core motifs with the desired optoelectronic properties. To that end, computational approaches such as those denoted by molecular docking studies are nowadays ubiquitous in providing insightful structural and enthalpic information regarding three-dimensional "weakly" bonded host−guest complexes, such as those formed between ligands and receptors in target proteins.[25,30,32,33] In molecular docking, each potential orientation of both the ligand and the receptor in the supramolecular complex is referred to as a pose. Poses are evaluated based on the ligand−protein affinity utilizing so-called scoring functions, where a "good score" is attributed to potentially successful binding interactions. In short, scoring functions can be broadly divided into knowledge-based scoring functions and energy component methods. The former are derived using the probability of known relevant intermolecular interactions from a large database. In turn, energy component methods denote scoring functions where the free energy (ΔG) following a supramolecular binding interaction process can be broken down into the sum of contributions such as the specific ligand−protein interactions as well as conformation changes upon binding.[35] However, in the quest to rationally develop novel sensing platforms for target analytes that exploit host−guest chemistries, knowledge of individual enthalpic contributions from amino acid residues would pave the way for the realization of superior technologies. Despite the large number of amino acid residues surrounding the ligands in the binding pocket of target proteins, the strength of the overall interaction is often uniquely dictated by a few key residues. These key amino acids can be called so due to exhibiting close interatomic distances with respect to the ligand and/or presenting appropriate relative orientations as to maximize the strength of the interaction.[35] In addition, on formation of the host−guest complex, both the binding pocket and ligand are likely to adopt an *ad hoc* conformation. The extent of those structural changes is also evaluated by scoring functions. As a result, an aspect of interest in molecular docking studies is the identification of biologically relevant conformations within the landscape of all possible three-dimensional arrangements. While relevant protein conformations can be afforded by means of protein X-ray crystallography, NMR studies, or more often, by homology modeling, the biological relevance of the yielded conformations of ligands denotes an ongoing debate within the molecular docking community[25,36] and can be partially ascribed to the intrinsically large structural flexibility of small molecules. In most cases and in the absence of crystallographic data, the geometries of ligands are obtained by following geometry optimization protocols using molecular mechanics, which are implemented in most commercially available molecular docking packages.[25,26,37] The latter, while denoting an appropriate approach for the rapid screening over a large data set of potential energy minima, lacks the accuracy of higher level quantum mechanics calculations.[25] Although in some cases, conformations of systems in the crystal structures of protein−ligand complexes are significantly less stable than energy minimum geometries,[38−40] access to experimentally determined crystallographic data of biologically relevant analytes is of paramount importance. This is particularly relevant in cases where crystallographic information is scarce, such as in the case of psychoactive substances.

Motivated by these shortcomings, herein, we report an in-depth *in silico* evaluation of the binding of psychoactive substances to target receptors in monoamine transporters,

https://dx.doi.org/10.1021/acsomega.0c01370
ACS Omega XXXX, XXX, XXX−XXX

particularly focused on the contributions of individual amino acid residues to such a binding event. Among the plethora of psychoactive substances, we selected MDAI, mexedrone, and phenibut in our study (Figure 2) based on their current

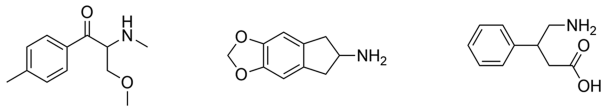

Figure 2. Chemical structures for mexedrone, MDAI, and phenibut.

relevance, the available literature, and their known interaction with the monoamine transporters.[22,41−45] To the best of our knowledge, this is the first study carrying out an in-depth investigation of the individual amino acid contributions to the overall binding interaction of psychoactive substances to receptors of those target proteins. To achieve that, we first optimized the geometries of the selected psychoactive substances (ligands) by means of molecular as well as quantum mechanics approaches and compared them to experimentally solved crystal structures to further understand their structural flexibility. Subsequently, the three optimized geometries for each ligand were docked against the three monoamine transporter proteins, namely, the DAT, the NET and the SERT. Evaluation of their docking scores highlights the critical impact of the conformation of the ligand, particularly in those structures with greater flexibility such as phenibut. Importantly, we observed that while the computed docking scores for the three MATs conformed to the experimentally determined potency trends for mexedrone, that was not the case for MDAI. With the aim of further investigating these observations and aiding in the rational design of superior point-of-care detection methodologies for psychoactive substances exploiting the modulation of the optoelectronic properties of the sensor upon interaction with the target analyte, we went on to quantify the individual contributions by means of quantum mechanics calculations. To do that, the three-dimensional coordinates of both ligands and receptors were extracted from the highest ranked poses and the intermolecular interactions of the psychoactive substance with each nearest neighboring amino acid residue calculated using a dimeric model. We observed that pharmacological trends were accounted for by our calculations in all cases. Importantly, in-depth evaluation of the individual amino acid contributions revealed the dominant role played by key amino acid residues, particularly those aromatic such as phenylalanine and tyrosine, in determining the strength of the binding and anticipate the importance of judiciously selecting peripheral substitutions in chemical sensors as well as core motifs to favor selective recognition. As a result, we believe this study to be of interest not only for those using computational approaches to understand protein−ligand interactions but more importantly, to the increasingly large community devoted to the development of superior point-of-care methodologies for biologically relevant analytes.

EXPERIMENTAL SECTION

Reagents and Materials. Hydrochloric acid was purchased from Fisher Scientific and used as received without any further purification. Reference standard materials (purity ≥98%) for mexedrone, MDAI, and phenibut were all purchased from Chiron AS (Trondheim, Norway) under UK Home Office License and used as supplied.

Preparation of Crystals for Single-Crystal X-ray Diffraction Analysis. Single crystals for mexedrone, MDAI, and phenibut were obtained by slow evaporation of cooled acidified (HCl) water solutions.

Crystal Structure Determination. All crystallographic measurements were made at 123(2) K with an Oxford Diffraction Gemini S diffractometer and monochromated Cu radiation (λ = 1.54184 Å). Programs from the SHELX suite were used for structure solution and refinement.[46] Refinement was to convergence against F^2 using all unique reflections. Non-H atoms were refined anisotropically. All H atoms bound to C were observed in difference maps but were included in the final model as riding atoms. The H atoms bound to O or to N were refined freely and isotropically. Selected crystallographic and refinement parameters are given in the Supporting Information (Table SI1.1). The crystal structure of mexedrone·HCl reported herein only exhibits small differences with respect to the one previously solved.[47] CCDC 1989619 to 1989621 contain the supplementary crystallographic data for this structure. These data can be obtained free of charge from the Cambridge Crystallographic Data Centre via www.ccdc.ac.uk/data_request/cif.

Molecular Docking Studies. Binding sites for all three monoamine transporters were elucidated utilizing the Molecular Operating Environment (MOE)[48] and then cross-referenced with the available literature to ensure that all residues considered to be important to binding were contained within the putative binding sites defined.[15,49] For the dopamine and norepinephrine transporters, the crystal structure of the Drosophila dopamine transporter in complex with the psychostimulant D-amphetamine (accession number 4XP9)[15] and cocaine (accession number 4XP4)[15] were used, respectively. The crystal structure of the ts3 human serotonin transporter complexed with *S*-citalopram at the central site and Br-citalopram at the allosteric site was used for the serotonin transporter (accession number 5I75).[49] Binding was carried out in the central site in all cases. Cavities were defined by probe radii 1 and 2 of 1.4 and 1.8 Å, respectively, a connection distance of 2.5 Å, and a minimum size of 3 residues.

Geometries for protonated forms of the three ligands were optimized by means of the MMFF94[50] force field as built in MOE's "quick-prep" methodology as well as the M06-2X[51] density functional at the 6-311G(d) level as implemented in Spartan '18 (v. 1.3.0),[52] without applying any constrains (Tables S2.1−S2.7). Geometries optimized with the latter were subjected to infrared analysis returning non-negative frequencies in all cases, consistent with a true equilibrium minimum.[37,53,54] It is noteworthy that the crystal structure conformation was selected as the starting point for the optimization by quantum mechanics. In turn, molecular mechanics optimization was carried out imputing the geometries as SMILES strings. Experimentally obtained crystal structure geometries were subjected to hydrogen atom optimization prior to docking studies following our previously reported method,[55] employing the M06-2X[51] density functional at the 6-311G(d) level as implemented in Spartan '18 (v. 1.3.0).[52] Single-point energies of the H-optimized crystal structure geometries as well as MMFF94-optimized systems were calculated at the M06-2X/6-311G(d) level for further comparison.

https://dx.doi.org/10.1021/acsomega.0c01370
ACS Omega XXXX, XXX, XXX−XXX

Protein models were prepared prior to inducing fit docking studies in MOE employing the MMFF94 force field.[50] Docking was carried out within the MOE package employing the triangle matcher placement method with a rigid receptor refinement to allow for a better comparison of the results for different geometries of the ligands. Poses were selected based on London ΔG and generalized-Born volume integral/weighted surface area (GWVI/WSA) energy component method scoring functions, with the number of docked poses generated set to a maximum of 30 or until the conformation of the ligand reached a default RMSD cutoff value of 3.0 Å.

Computation of Intermolecular Interactions. MOE-induced fit docking outputs (coordinates) were extracted for all investigated protein−ligand complexes and nearest neighbor amino acid residues selected using an interatomic distance cutoff value of 4.5 Å. Binding energies between each ligand and the nearest neighbor amino acid residues were then calculated within the framework of a dimeric model by means of Truhlar's density functional M06-2X[51] at the 6-311G(d) level as implemented in Spartan '18 (v.1.3.0) software.[52] All computed intermolecular interactions were corrected for basis set superposition error (BSSE) by means of the counterpoise method of Boys and Bernardi.[56]

RESULTS AND DISCUSSION

Structural Flexibility of the Ligands. Most small molecules are intrinsically characterized by a large structural flexibility, which inevitably leads to concerns when trying to obtain biologically relevant conformations for docking studies.[25,38] It is noteworthy that in some cases, experimentally determined conformations by means of X-ray crystallography are significantly less stable than the geometry at the global minimum and in some cases do not even correspond to geometries at local minima.[38−40] However, these are critical in the assessment of computationally optimized geometries. As a result, we deemed of interest to investigate in detail the yielded ligand conformations that the three psychoactive substances exhibit by means of commonly used molecular mechanics protocols implemented in commercial molecular docking software with those obtained by means of quantum mechanics calculations as well as X-ray crystallographic studies. For all three protonated ligands, namely, mexedrone, MDAI, and phenibut, we report molecular mechanics as well as experimental crystal structure geometries, which are less stable than their conformations yielded by quantum mechanics calculations. In short, while the differences with the crystal structures can be attributed to interactions with neighboring monomers as well as solvent molecules during the crystal growth process as opposed to quantum mechanics calculations, the comparison with molecular mechanics-yielded geometries could be associated with starting conformations in those calculations.

In the case of both MDAI and mexedrone, the largest differences were observed between quantum and molecular mechanics optimized conformations (ΔE = 24.85 kJ mol^{-1}) and between optimized quantum mechanics and experimental crystal structure geometries (ΔE = 24.53 kJ mol^{-1}), respectively. Interestingly, we compute a significantly less stable molecular mechanics conformation of phenibut when compared to its crystal structure counterpart (ΔE = 86.84 kJ mol^{-1}) and to a greater extent with respect to its quantum mechanics counterpart (ΔE = 110.07 kJ mol^{-1}). In some cases, large conformational reorganization energies can be attributed to variations in bond lengths between the two geometries.[57] However, here, detailed analysis of the variations in bond lengths for all investigated ligands reveals no significant changes that could account for the observed energy differences between conformations. Instead, we observed that unlike for the different yielded conformations for MDAI and mexedrone, the optimized geometry of phenibut by means of molecular mechanics exhibits a critical structural difference with respect to the quantum mechanics-optimized geometry as well as experimental crystal structure geometry as illustrated in Figure 3. It should be noted that the geometry of the crystal structure

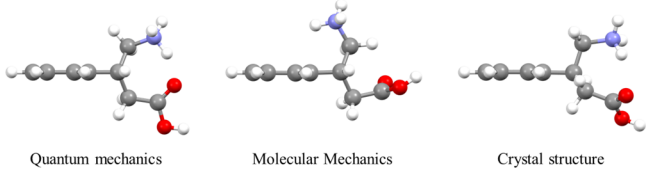

Figure 3. Phenibut conformations yielded by quantum mechanics optimization (left), docking studies using molecular mechanics (center), and crystal structure (right).

was utilized as the starting point in quantum mechanics geometry optimization calculations, whereas molecular mechanics geometry optimizations were performed from SMILES strings inputs, hence lacking three-dimensional information.

Figure 3 illustrates the conformations of phenibut yielded for the three different approaches utilized in this work. The conformations particularly differ on the orientation of the protonated amine with respect to the plane of the benzene ring, with the crystal structure and quantum mechanics geometries exhibiting an exo-type conformation of the amine group with measured dihedral angles of θ = 178.26 and 148.93°, respectively. In turn, the optimized geometry by molecular mechanics from SMILES strings is characterized by an endo-type conformation (θ = 50.72°) where the amine is closely situated above the plane of the benzene ring, which we anticipate could lead to a reduced number of intermolecular interactions with neighboring amino acid residues. As a result, we investigated this further. It could be argued that the conformation obtained by molecular mechanics denotes local minima situated in a different region to that of the energy minima yielded by quantum mechanics, along the potential energy surface. To further evaluate this observation, we went on optimizing the molecular mechanics geometry by means of quantum mechanics. We observed that the newly optimized geometry (Table S2.5) exhibits no negative frequencies on the computed infrared spectrum and hence conforms to the geometry of energy minima. The resulting conformation, similar to the case of its molecular mechanics counterpart, is characterized by an endo-type arrangement of the amine with respect to the benzene ring (θ = 51.59°). As a result, these findings highlight the importance of evaluating the conformations of ligands, particularly in molecular docking studies. In the following, we examine in detail the docking scores obtained for the different conformations of the three investigated psychoactive substances in their target proteins.

Molecular Docking Studies. The ability of the three psychoactive substances to interact with plasma membrane monoamine transporters was investigated using molecular docking studies. In all cases, the geometries of both ligands and proteins were kept rigid upon binding to facilitate further

https://dx.doi.org/10.1021/acsomega.0c01370
ACS Omega XXXX, XXX, XXX−XXX

evaluation of any structural causation to the interaction process. Yielded poses were rank-ordered employing their docking scores, with the following analysis focusing on the top ranked pose for each conformation evaluated (Tables S3.1−S3.9).

In agreement with previous studies,[15,49] we report that in all investigated cases and irrespective of the rank order of the pose, the preferred binding site was the so-called central or S1 site, which in the case of the serotonin transporter is located between helices 1, 3, 6, 8, and 10.[49] Table 1 summarizes the docking scores for the highest ranked poses for the different evaluated conformations of each psychoactive substance in all three monoamine transporters.

Table 1. Computed Docking Scores for the Highest Ranked Poses for the Different Ligand Geometries in All Investigated Monoamine Transporters (MATs)

ligand	conformation	MAT	docking score
MDAI	quantum mechanics	DAT	−5.5362
		NET	−5.7010
		SERT	−5.0285
	molecular mechanics	DAT	−5.5082
		NET	−5.6839
		SERT	−4.9237
	crystal structure	DAT	−5.5249
		NET	−5.6946
		SERT	−5.0389
mexedrone	quantum mechanics	DAT	−5.7706
		NET	−5.6254
		SERT	−5.1283
	molecular mechanics	DAT	−4.8010
		NET	−4.8016
		SERT	−5.8647
	crystal structure	DAT	−4.3128
		NET	−5.9837
		SERT	−4.9222
phenibut	quantum mechanics	DAT	−4.8739
		NET	−5.5350
		SERT	−4.6779
	molecular mechanics	DAT	−4.3116
		NET	−5.3696
		SERT	−5.1323
	crystal structure	DAT	−5.5775
		NET	−5.3073
		SERT	−4.9307

Careful analysis of these results reveal that different ligand conformations have a negligible impact on the computed docking scores for the top poses of MDAI-containing complexes, which can be attributed to the small flexibility of this psychoactive substance when compared to mexedrone and phenibut (vide supra). Our computational docking results indicate that, in agreement with experimental studies,[19,58] MDAI acts on all three monoamine transporters. However, the often-observed higher potency of MDAI on the NET and the SERT when compared to that on the DAT is not fully accounted for by our docking results, hence warranting further computational studies on the docking of this psychoactive substance. This is particularly interesting given the large structural similarity between the DAT and the NET.[15,49] In this regard, evaluation of the position of the ligand exhibiting the crystal structure geometry within the cavity of the central binding site of the three MATs is consistent with small differences in the scoring values for docking onto the DAT and the NET, attributed to a similar sequence of nearest neighboring amino acids bordering the ligand. Although scoring factors consider other aspects of the binding process and not just the intermolecular interactions, the latter can be associated with fewer and longer distance interactions with amino acid residues when compared to docking on the other transporters and will be accordingly analyzed in depth in the following section.

The highest ranked poses for mexedrone and phenibut docking on the MATs do, on the contrary, exhibit docking scores, which vary according to the conformation used. This can be ascribed to their larger structural flexibility and the observed conformational changes upon optimization/experimental crystal growth, particularly in the case of phenibut. In line with our previous observations on the structural variations for the different conformers of phenibut, we report these to bear a greater impact on the yielded docking scores for the DAT (S = −4.8739, −5.5775, and −4.1316 for quantum mechanics, crystal structure, and molecular mechanics geometries, respectively). In fact, the docking score for the molecular mechanics-optimized geometry was computed to be the lowest for all investigated ligand−MAT pairs. Underpinned by the detailed structural analysis of the different yielded conformations of the ligands, we associate this finding with the observed endo-type arrangement of the protonated amine with respect to the benzene core, hence resulting in fewer intermolecular contacts with bordering amino acid residues.

While, to the best of our knowledge, there is a lack of pharmacological studies on the interactions of phenibut with the monoamine transporters, experimental observations made for mexedrone interactions indicate higher potency values for the NET.[47] Along those lines, it is of note that our computed docking scores employing the geometry of the crystal structure (Table 1) are in agreement with these observations, whereas scoring values for the conformations obtained following the molecular docking protocol do not conform to the experimental observations. Furthermore, the score for the docking of the crystal structure conformation of mexedrone onto the NET is the highest we report for all investigated systems, largely attributed to close intermolecular interactions with phenylalanine (43, 319, and 325) residues (Figures S4.58−S4.60).

In light of these findings and to aid the development of superior sensing platforms for these psychoactive substances exploiting host−guest type chemistries, in the following, we will explore in detail the determined intermolecular interactions between the crystal structure geometries for each ligand and nearest neighbor amino acid residues in all three monoamine transporters.

Intermolecular Interactions, ΔE_{CP}. Intermolecular interaction energies were computed for the binding of the crystal structure geometries of the psychoactive substances and nearest neighboring amino acid residues in each monoamine transporter, which were obtained from molecular docking studies. First, we deemed of interest to compare the order of the docking scores, which are calculated based on different contributions and not solely the strength of the interaction, with that of the overall computed intermolecular interaction in each evaluated case, $\Sigma\Delta E_{CP}$. It is noteworthy that for the two psychoactive substances for which pharmacological data is available, namely, MDAI and mexedrone, our computed

https://dx.doi.org/10.1021/acsomega.0c01370
ACS Omega XXXX, XXX, XXX−XXX

intermolecular interactions conform to the potency trends observed experimentally for the three MATs. While docking studies were also in agreement with experimental data in relation to the activity of mexedrone, this was not the case for the aminoindane MDAI for which docking results predicted the highest potency on the NET (Table 1). In turn, $\Sigma\Delta E_{CP}$ results are consistent with experimental studies, which reveal greater activity on the SERT, thus highlighting the importance of the approach proposed herein. Predicted trends employing computed intermolecular interactions for phenibut agree with those obtained by molecular docking (vide supra).

Table 2 summarizes the computed intermolecular interactions for MDAI with nearest neighbor amino acid residues in all three monoamine transporters. Interestingly, despite the different orientation of MDAI within the pocket of the DAT and the NET, we identified that 10 out of the 12 nearest neighbors that facilitate binding to the NET were also present in the complex with the DAT, albeit exhibiting different computed intermolecular interactions as a result of the distinct relative three-dimensional orientation (ΔE_{CP} (Ala 117) = −8.84 and −76.81 kJ mol^{-1} for DAT and NET, respectively). In addition, none of these particular amino acid residues contributes to the large computed binding of MDAI to the SERT ($\Sigma\Delta E_{CP}$ = −266.04 kJ mol^{-1}).

Table 2. Computed Counterpoise-Corrected Intermolecular Interactions, ΔE_{CP} (kJ mol^{-1}), for MDAI with Nearest Neighboring Amino Acid Residues within the Binding Sites of the DAT, NET, and SERT Monoamine Transporters (Figures S4.1−S4.34)

DAT		NET		SERT	
amino acid	ΔE_{CP}	amino acid	ΔE_{CP}	amino acid	ΔE_{CP}
Ala 117	−8.84	Ala 117	−76.81	Ala 96	−44.76
Asp 46	21.53	Asn 125	−11.59	Asp 98	20.15
Asp 121	−13.89	Asp 46	6.32	Gly 338	5.60
Gly 425	3.57	Asp 121	−3.87	Gly 442	−3.25
Phe 43	−44.65	Gly 425	−6.86	Ile 172	−2.87
Phe 319	−52.99	Phe 43	−12.69	Phe 335	−54.61
Phe 325	−9.35	Phe 325	−22.21	Phe 341	−3.23
Ser 421	−5.16	Ser 421	−7.20	Ser 336	−39.33
Ser 422	−6.70	Ser 422	−23.12	Ser 438	−6.55
Tyr 124	−28.32	Ser 426	−13.92	Tyr 95	−122.46
Val 120	−13.97	Tyr 124	−16.39	Tyr 176	−14.73
		Val 120	−24.91		

In fact, we report the largest overall intermolecular interactions for the binding of MDAI to the SERT, with noteworthy stabilizing contributions from Ala 96 (ΔE_{CP} = −44.76 kJ mol^{-1}), Phe 335 (ΔE_{CP} = −54.61 kJ mol^{-1}), and especially Tyr 95 (ΔE_{CP} = −122.46 kJ mol^{-1}) residues, all of which exhibit interactions that engage their electronegative carbonyl oxygen atoms and positively charged amine of the ligand (Figure 4). The observed greater interaction with the Tyr 95 residue can be further associated with (i) the closer distance of the previously described interaction and (ii) the additional T-shape-type interaction between the phenylalanine phenol and the MDAI core. The latter finding exemplifies that while selectivity toward a particular analyte in the design of chemical sensors via judicious selection of peripheral substitutions is appropriate, adequate selection of core motifs also plays a critical role.

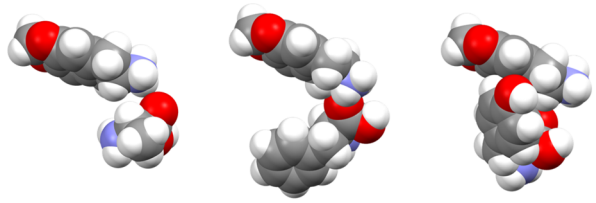

Figure 4. Spacefill illustration of the interaction between MDAI and Ala 96 (left), Phe 335 (center), and Tyr 95 (right) residues in the binding to the SERT.

Similar to the observations made for the binding of MDAI, we observe a large number of common amino acid residues (11 out of 14 nearest neighbor NET residues) responsible for the interaction of mexedrone within the central cavity of the DAT and the NET. Despite the latter, there are significant differences in the overall computed strength of the binding of the ligand to those monoamine transporters. While we compute mexedrone having the largest interaction energy to the NET, we report the lowest value for the DAT, with the overall interaction to the SERT somewhere in between ($\Sigma\Delta E_{CP}$ = −105.20, −182.53, and −158.53 kJ mol^{-1} for binding to the DAT, the NET, and the SERT, respectively). The approximately 2-fold increase in the $\Sigma\Delta E_{CP}$ on progression from the DAT to the NET can be particularly associated with the contributions of two amino acid residues, namely, Asp 46 and Phe 43. In evaluating this finding, we observed that the large destabilizing interaction of mexedrone with Asp 46 in the binding to the DAT, which can be associated with a close contact between the electropositive aspartic hydrogen atom of the acid group and the protonated amine of the ligand, becomes almost negligible on binding to the NET (ΔE_{CP} (Asp 46) = 28.76 and 2.48 kJ mol^{-1} for DAT and NET, respectively). On the contrary, the stabilizing energy computed for the mexedrone−Phe 43 pair in the DAT (ΔE_{CP} = −24.44 kJ mol^{-1}) was observed to increase significantly in the case of the binding within the NET S1 site (ΔE_{CP} = −59.10 kJ mol^{-1}). We attribute the latter to the synergistic contribution of the interaction between the electropositive amine hydrogen atom and the electronegative carbonyl oxygen at 2.625 Å as well as the stabilizing interaction of the protonated mexedrone amine with the phenylalanine core (Table 3).

Lastly, we focus on the individual amino acid contributions on the binding of phenibut to the different monoamine transporters. In contrast to the observations made for the other two psychoactive substances where the lowest interactions were computed for the binding to the DAT, we report the largest overall interaction for phenibut when docked to this monoamine transporter ($\Sigma\Delta E_{CP}$ = −172.07, −117.37, and −153.45 kJ mol^{-1} for binding to the DAT, the NET, and the SERT, respectively). Upon judicious analysis of the binding of the three ligands to the dopamine monoamine transporter, we attribute the larger interaction energy of phenibut ($\Sigma\Delta E_{CP}$ = −158.77, −105.20, and − 172.07 kJ mol^{-1} for binding of MDAI, mexedrone, and phenibut to the DAT, respectively) to (i) a decrease of the destabilizing interaction with an aspartic acid residue (Asp 46) and (ii) the increase of the binding interaction to a tyrosine residue (Tyr 124) Figure 5.

In relation to the differences in the computed intermolecular interactions between the psychoactive substances and the Asp

https://dx.doi.org/10.1021/acsomega.0c01370
ACS Omega XXXX, XXX, XXX−XXX

Table 3. Computed Counterpoise-Corrected Intermolecular Interactions, ΔE_{CP} (kJ mol^{-1}), for Mexedrone with Nearest Neighboring Amino Acid Residues within the Binding Sites of the DAT, NET and SERT Monoamine Transporters (Figures S4.35−S4.74)

DAT		NET		SERT	
amino acid	ΔE_{CP}	amino acid	ΔE_{CP}	amino acid	ΔE_{CP}
Ala 44	−16.46	Ala 44	−12.72	Asp 98	6.1447
Ala 48	3.01	Ala 117	−9.05	Glu 493	−68.37
Asp 46	28.76	Asp 46	2.48	Ile 172	−4.22
Asp 121	−5.72	Asp 121	−1.28	Phe 335	−22.84
Gly 322	−1.46	Gly 322	−2.82	Ser 438	−6.08
Gly 425	6.84	Gly 452	2.22	Thr 497	−15.74
Leu 321	−8.35	Leu 321	−9.04	Tyr 95	−20.49
Phe 43	−24.44	Phe 43	−59.10	Tyr 175	−16.03
Phe 319	−50.63	Phe 319	−32.44	Tyr 176	−13.08
Phe 325	2.22	Phe 325	−18.64	Val 501	2.18
Ser 320	−5.33	Ser 320	−21.18		
Ser 421	−6.11	Ser 421	0.45		
Ser 422	2.71	Tyr 124	−12.77		
Tyr 124	−22.54	Val 120	−8.64		
Val 120	−7.70				

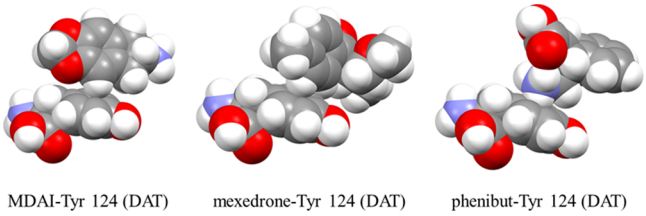

Figure 5. Spacefill representation of the interaction MDAI (left), mexedrone (center), and phenibut (right) with the Tyr 124 residue within the S1 site of the DAT.

46 residue (ΔE_{CP} = 21.53, 28.76, and 4.01 kJ mol^{-1} for binding of MDAI, mexedrone, and phenibut to the Asp 46 residue, respectively), these can be accounted for by means of the greater interaction distance in the case of the binding to phenibut as a result of a different three-dimensional arrangement of the ligand within the central cavity of the transporter. Likewise, the observed approximately 2-fold increase in the stabilizing intermolecular interaction computed for the binding the ligands to the tyrosine (Tyr 124) on progression from MDAI and mexedrone to Phenibut (ΔE_{CP} = −28.32, −22.54, and − 57.07 kJ mol^{-1} for binding of MDAI, mexedrone and phenibut to the Tyr 124 residue, respectively) can also be attributed to critical changes in the relative ligand−receptor orientation within the S1 site of the DAT. In this case, we observe that while binding of both MDAI and mexedrone is facilitated by close T-shape interaction between aromatic moieties of the ligands and the benzene core of the residue, the increase in the computed ΔE_{CP} is associated with protonated phenibut amine with the core of the amino acid (Table 4).

CONCLUSIONS

In conclusion, the binding of topical psychoactive substances such as MDAI, mexedrone, and phenibut to the monoamine transporters for dopamine, norepinephrine, and serotonin was investigated to aid in the development of superior sensing platforms for these target analytes that exploit host−guest type chemistries. To do that and in light of the known structural

Table 4. Computed Counterpoise-Corrected Intermolecular Interactions, ΔE_{CP} (kJ mol^{-1}), for Phenibut with Nearest Neighboring Amino Acid Residues within the Binding Sites of the DAT, NET, and SERT Monoamine Transporters (Figures S4.75−S4.112)

DAT		NET		SERT	
amino acid	ΔE_{CP}	amino acid	ΔE_{CP}	amino acid	ΔE_{CP}
Ala 44	−0.65	Ala 44	−9.04	Ala 96	−27.69
Ala 117	−15.48	Ala 48	3.74	Asp 98	8.65
Asp 46	4.01	Asp 46	−5.14	Gly 338	−0.38
Gly 332	−3.05	Phe 43	−29.19	Gly 442	−0.15
Gly 425	4.53	Phe 319	−9.69	Ile 172	−4.62
Leu 321	−9.59	Phe 325	−18.64	Leu 337	−1.23
Phe 43	−33.13	Ser 320	−21.19	Phe 335	−50.92
Phe 319	−15.16	Ser 421	−6.99	Phe 341	−7.74
Phe 325	−7.22	Ser 422	0.18	Ser 336	−13.41
Ser 320	−8.17	Tyr 124	−12.77	Ser 438	−3.18
Ser 421	−4.12	Val 120	−8.64	Tyr 95	−33.68
Ser 422	−4.13			Tyr 176	−21.34
Tyr 124	−57.07			Val 97	2.24
Val 120	−22.84				

flexibility of most ligands and prior to docking studies, we evaluated the conformational changes of optimized geometries of the psychoactive substances by means of quantum as well as molecular mechanics and compare them to experimentally determined crystal structure geometries. Interestingly, in the case of phenibut, it was observed that the molecular mechanics-optimized geometry using SMILES string input leads to a critically different conformer, where the endo-type position of the protonated amine contrasts with the exo orientation observed in the crystal structure and quantum mechanics-optimized geometries. All conformers for each ligand were then docked against target receptors using molecular docking approaches. We observed that in the case of MDAI, docking results for top ranked poses were influenced by the conformation of the ligand and that experimentally determined trends for the three transporters were not well predicted by the computational methodologies. In turn, computational trends obtained for the crystal structure conformation of mexedrone conformed to experimental observations, with a higher affinity for the interaction with the NET. Subsequently, these results were further evaluated by determining the intermolecular interactions between the crystal structure geometries of the ligands and their nearest neighbor amino acid residues in each monoamine transporter. We found that the overall interaction energy computed for MDAI was in agreement with experimental observations and that the computed trends for mexedrone were further ratified. In all cases, overall binding energies were rationally narrowed down to contributions with key amino acids, which would be critical in guiding the development of superior chemical sensors. In particular, the greater interaction of MDAI with the DAT when compared to that computed for its counterparts, mexedrone and phenibut, was attributed to lower destabilization upon interaction with the aspartic acid (46) residue and more importantly to the strengthening of the interaction with the tyrosine (124) residue within the S1 site of the transporter. As a result, we believe the approach herein detailed to be of interest for those engaged in the *in silico* evaluation of protein−ligand interactions and to furthermore be invaluable in the development of novel chemical sensors for biologically relevant

https://dx.doi.org/10.1021/acsomega.0c01370
ACS Omega XXXX, XXX, XXX−XXX

analytes via judicious selection of peripheral substitutions performed on core motifs with the desired optoelectronic properties.

■ ASSOCIATED CONTENT

Supporting Information

The Supporting Information is available free of charge at https://pubs.acs.org/doi/10.1021/acsomega.0c01370.

Selected crystallographic and refinement parameters for the three crystal structures (SI1), Cartesian coordinates for the optimized geometries of the monomers (SI2), full details for the docking studies (SI3), and capped stick illustrations of all ligand−amino acid dimers (SI4) (PDF)

■ AUTHOR INFORMATION

Corresponding Author

Jesus Calvo-Castro − *School of Life and Medical Sciences, University of Hertfordshire, Hatfield AL10 9AB, U.K.;* orcid.org/0000-0003-1031-8648; Email: j.calvo-castro@herts.ac.uk

Authors

Tamara Senior − *School of Life and Medical Sciences, University of Hertfordshire, Hatfield AL10 9AB, U.K.*

Michelle J. Botha − *School of Life and Medical Sciences, University of Hertfordshire, Hatfield AL10 9AB, U.K.*

Alan R. Kennedy − *Department of Pure & Applied Chemistry, University of Strathclyde, Glasgow G1 1XL, U.K.;* orcid.org/0000-0003-3652-6015

Complete contact information is available at: https://pubs.acs.org/10.1021/acsomega.0c01370

Notes

The authors declare no competing financial interest.

■ ACKNOWLEDGMENTS

J.C.C. acknowledges funding for T.S. from the University of Hertfordshire.

■ REFERENCES

(1) Howell, L. L.; Kimmel, H. L. Monoamine Transporters and Psychostimulant Addiction. *Biochem. Pharmacol.* **2008**, *75*, 196−217.

(2) Solich, J.; Kolasa, M.; Kusmider, M.; Faron-Gorecka, A.; Pabian, P.; Zurawek, D.; Szafran-Pilch, K.; Dziedzicka-Wasylewska, M. Norepinephrine Transporter Knock-out Alters Expression of the Genes Connected with Antidepressant Drugs Action. *Brain Res.* **2015**, *1594*, 284−292.

(3) Bröer, S.; Gether, U. The Solute Carrier 6 Family of Transporters. *Br. J. Pharmacol.* **2012**, *167*, 256−278.

(4) Kristensen, A. S.; Andersen, J.; Jørgensen, T. N.; Sørensen, L.; Eriksen, J.; Loland, C. J.; Strømgaard, K.; Gether, U. SLC6 Neurotransmitter Transporters: Structure, Function, and Regulation. *Pharmacol. Rev* **2011**, *63*, 585−640.

(5) Lin, Z.; Canales, J. J.; Björgvinsson, T.; Thomsen, M.; Qu, H.; Liu, Q.-R.; Torres, G. E.; Caine, S. B. Monoamine Transporters: Vulnerable and Vital Doorkeepers; *Progress in Molecular Biology and Translational Science*; Academic Press, 2011; Vol. *98*, DOI: 10.1016/B978-0-12-385506-0.00001-6.

(6) Rothman, R. B.; Baumann, M. H.; Prisinzano, T. E.; Newman, A. H. Dopamine Transport Inhibitors Based on GBR12909 and Benztropine as Potential Medications to Treat Cocaine Addiction. *Biochem. Pharmacol.* **2008**, *75*, 2−16.

(7) Torres, G. E.; Gainetdinov, R. R.; Caron, M. G. Plasma Membrane Monoamine Transporters: Structure Regulation and Function. *Nat. Rev. Neurosci.* **2003**, *4*, 13−25.

(8) Reith, M. E. A.; Blough, B. E.; Hong, W. C.; Jones, K. T.; Schmitt, K. C.; Baumann, M. H.; Partilla, J. S.; Rothman, R. B.; Katz, J. L. Behavioral, Biological, and Chemical Perspectives on Atypical Agents Targeting the Dopamine Transporter. *Drug Alcohol Depend.* **2015**, *147*, 1−19.

(9) Vaughan, R. A.; Foster, J. D. Mechanisms of Dopamine Transporter Regulation in Normal and Disease States. *Trends Pharmacol. Sci.* **2013**, *34*, 489−496.

(10) Olivier, B. Serotonin: A Never-Ending Story. *Eur. J. Pharmacol.* **2015**, *753*, 2−18.

(11) Sitte, H. H.; Freissmuth, M. Amphetamines, New Psychoactive Drugs and the Monoamine Transporter Cycle. *Trends Pharmacol. Sci.* **2015**, *36*, 41−50.

(12) Zhou, Z.; Zhen, J.; Karpowich, N. K.; Law, C. J.; Reith, M. E. A.; Wang, D.-N. Antidepressant Specificity of Serotonin Transporter Suggested by Three LeuT-SSRI Structures. *Nat. Struct. Mol. Biol.* **2009**, *16*, 652−657.

(13) Wang, C.-I. A.; Shaikh, N. H.; Ramu, S.; Lewis, R. J. A Second Extracellular Site Is Required for Norepinephrine Transport by the Human Norepinephrine Transporter. *Mol. Pharmacol.* **2012**, *82*, 898−909.

(14) Borgkvist, A.; Malmlöf, T.; Feltmann, K.; Lindskog, M.; Schilström, B. Dopamine in the Hippocampus Is Cleared by the Norepinephrine Transporter. *Int. J. Neuropsychopharmacol.* **2011**, *15*, 531−510.

(15) Penmatsa, A.; Wang, K. H.; Gouaux, E. X-Ray Structures of Drosophila Dopamine Transporter in Complex with Nisoxetine and Reboxetine. *Nat. Struct. Mol. Biol.* **2015**, *22*, 506−508.

(16) Daws, L. C. Unfaithful Neurotransmitter Transporters: Focus on Serotonin Uptake and Implications for Antidepressant Efficacy. *Pharmacol. Ther.* **2009**, *121*, 89−99.

(17) Larsen, M. B.; Sonders, M. S.; Mortensen, O. V.; Larson, G. A.; Zahniser, N. R.; Amara, S. G. Dopamine Transport by the Serotonin Transporter: A Mechanistically Distinct Mode of Substrate Translocation. *J. Neurosci.* **2011**, *31*, 6605−6615.

(18) Green, A. R.; Mechan, A. O.; Elliott, J. M.; O'Shea, E.; Colado, M. I. The Pharmacology and Clinical Pharmacology of 3,4-Methylenedioxymethamphetamine (MDMA, "Ecstasy"). *Pharmacol. Rev.* **2003**, *55*, 463−508.

(19) Hysek, C. M.; Simmler, L. D.; Schillinger, N.; Meyer, N.; Schmid, Y.; Donzelli, M.; Grouzmann, E.; Liechti, M. E. Pharmacokinetic and Pharmacodynamic Effects of Methylphenidate and MDMA Administered Alone or in Combination. *Int. J. Neuropsychopharmacol.* **2014**, *17*, 371−381.

(20) Berridge, K. C.; Kringelbach, M. L. Pleasure Systems in the Brain. *Neuron* **2015**, *86*, 646−664.

(21) UNODC. *UNODC. 2018. Understanding the Synthetic Drug Market: NPS Factor*. Vienna: United Nations on Drug and Crime. 2018.

(22) Dargan, P. I.; Wood, D. M. *Novel Psychoactive Substances: Classification, Pharmacology and Toxicology*; Elsevier, 2013.

(23) Iversen, L.; Gibbons, S.; Treble, R.; Setola, V.; Huang, X.-P.; Roth, B. L. Neurochemical Profiles of Some Novel Psychoactive Substances. *Eur. J. Pharmacol.* **2013**, *700*, 147−151.

(24) Smith, J. P.; Sutcliffe, O. B.; Banks, C. E. An Overview of Recent Developments in the Analytical Detection of New Psychoactive Substances (NPSs). *Analyst* **2015**, *140*, 4932−4948.

(25) Shim, J.; MacKerell, A. D. J. Computational Ligand-Based Rational Design: Role of Conformational Sampling and Force Fields in Model Development. *MedChemComm* **2011**, *2*, 356−370.

(26) Leach, A. R.; Gillet, V. J.; Lewis, R. A.; Taylor, R. Three-Dimensional Pharmacophore Methods in Drug Discovery. *J. Med. Chem.* **2010**, *53*, 539−558.

(27) Langer, T.; Hoffmann, R. D. *Pharmacophores and Pharmacophore Searches*; Pharmacophores and Pharmacophore Searches; 2006, DOI: 10.1002/3527609164.

(28) Kellett, K.; Broome, J. H.; Zloh, M.; Kirton, S. B.; Fergus, S.; Gerhard, U.; Stair, J. L.; Wallace, K. J. Small Molecule Recognition of Mephedrone Using an Anthracene Molecular Clip. *Chem. Commun.* **2016**, *52*, 7474−7477.
(29) Černý, J.; Hobza, P. Non-Covalent Interactions in Biomacromolecules. *Phys. Chem. Chem. Phys.* **2007**, *9*, 5291−5303.
(30) Ronconi, L.; Sadler, P. J. Using Coordination Chemistry to Design New Medicines. *Coord. Chem. Rev.* **2007**, *251*, 1633−1648.
(31) Hobza, P. Calculations on Noncovalent Interactions and Databases of Benchmark Interaction Energies. *Acc. Chem. Res.* **2012**, *45*, 663−672.
(32) Calvo-Castro, J.; McHugh, C. J. Exploring Structure Based Charge Transport Relationships in Phenyl Diketopyrrolopyrrole Single Crystals Using a 2D π- π Dimer Model System. *J. Mater. Chem. C* **2017**, *5*, 3993−3998.
(33) Steiner, T.; Desiraju, G. R. Distinction between the Weak Hydrogen Bond and the van Der Waals Interaction. *Chem. Commun.* **1998**, *8*, 891−892.
(34) Chung, S. J.; McHugh, C. J.; Calvo-Castro, J. A 2-D π-π Dimer Model System to Investigate Structure-Charge Transfer Relationships in Rubrene. *J. Mater. Chem. C* **2019**, *7*, 2029−2036.
(35) Kroemer, R. T. Structure-Based Drug Design: Docking and Scoring. *Curr. Protein Pept Sci.* **2007**, *8*, 312−328.
(36) Levoin, N.; Calmels, T.; Krief, S.; Danvy, D.; Berrebi-Bertrand, I.; Lecomte, J.-M.; Schwartz, J.-C.; Capet, M. Homology Model Versus X-Ray Structure in Receptor-Based Drug Design: A Retrospective Analysis with the Dopamine D3 Receptor. *ACS Med. Chem. Lett.* **2011**, *2*, 293−297.
(37) Leach, A. R. *Molecular Modelling. Principles and Applications*; Prentice-Hall, Ed.; Prentice-Hall, 2001.
(38) Perola, E.; Charifson, P. S. Conformational Analysis of Drug-Like Molecules Bound to Proteins: An Extensive Study of Ligand Reorganization upon Binding. *J. Med. Chem.* **2004**, *47*, 2499−2510.
(39) Agrafiotis, D. K.; Gibbs, A. C.; Zhu, F.; Izrailev, S.; Martin, E. Conformational Sampling of Bioactive Molecules: A Comparative Study. *J. Chem. Inf. Model.* **2007**, *47*, 1067−1086.
(40) Foloppe, N.; Chen, I.-J. Conformational Sampling and Energetics of Drug-like Molecules. *Curr. Med. Chem.* **2009**, *16*, 3381−3413.
(41) Qian, Z.; Jia, W.; Li, T.; Liu, C.; Hua, Z. Identification and Analytical Characterization of Four Synthetic Cathinone Derivatives Iso-4-BMC, β-TH-Naphyrone, Mexedrone, and 4-MDMC. *Drug Test. Anal.* **2017**, *9*, 274−281.
(42) Lapin, I. Phenibut (β-Phenyl-GABA): A Tranquilizer and Nootropic Drug. *CNS Drug Rev.* **2001**, *7*, 471−481.
(43) Brandt, S. D.; Braithwaite, R. A.; Evans-Brown, M.; Kicman, A. T. Chapter 11- Aminoindane Analogues. In *Novel Psychoactive Substances*; Wood, P. I. D. M., Ed.; Academic Press: Boston, 2013; pp 261−283.
(44) Sainsbury, P. D.; Kicman, A. T.; Archer, R. P.; King, L. A.; Braithwaite, R. A. Aminoindanes-the next Wave of "Legal Highs"? *Drug Test. Anal.* **2011**, *3*, 479−482.
(45) Jin, H.; Kim, S. T.; Hwang, G.-S.; Ryu, D. H. L -Proline Derived Bifunctional Organocatalysts: Enantioselective Michael Addition of Dithiomalonates to Trans-β-Nitroolefins. *J. Org. Chem.* **2016**, *81*, 3263−3274.
(46) Sheldrick, G. M. A Short History of SHELX. *Acta Crystallogr. Sect. A* **2008**, *64*, 112−122.
(47) McLaughlin, G.; Morris, N.; Kavanagh, P. V.; Power, J. D.; Dowling, G.; Twamley, B.; O'Brien, J.; Talbot, B.; Walther, D.; Partilla, J. S.; Baumann, M. H.; Brandt, S. D. Synthesis, Characterization and Monoamine Transporter Activity of the New Psychoactive Substance Mexedrone and Its N-Methoxy Positional Isomer, N-Methoxymephedrone. *Drug Test. Anal.* **2017**, *9*, 358−368.
(48) Chemical Computing Group Inc. *Molecular Operating Environment (MOE)*; Chemical Computing Group Inc: Montreal, QC, Canada, 2014.
(49) Coleman, J. A.; Green, E. M.; Gouaux, E. X-Ray Structures and Mechanism of the Human Serotonin Transporter. *Nature* **2016**, *532*, 334−339.
(50) Halgren, T. A.; Nachbar, R. B. Merck Molecular Force Field. IV. Conformational Energies and Geometries for MMFF94. *J. Comput. Chem.* **1996**, *17*, 587−615.
(51) Zhao, Y.; Truhlar, D. G. The M06 Suite of Density Functionals for Main Group Thermochemistry, Thermochemical Kinetics, Noncovalent Interactions, Excited States, and Transition Elements: Two New Functionals and Systematic Testing of Four M06-Class Functionals and 12 Other Functionals. *Theor. Chem. Acc.* **2008**, *120*, 215−241.
(52) Shao, Y.; Molnar, L. F.; Jung, Y.; Kussmann, J.; Ochsenfeld, C.; Brown, S. T.; Gilbert, A. T. B.; Slipchenko, L. V.; Levchenko, S. V.; O'Neill, D. P.; DiStasio, R. A., Jr.; Lochan, R. C.; Wang, T.; Beran, G. J. O.; Besley, N. A.; Herbert, J. M.; Lin, C. Y.; Van Voorhis, T.; Chien, S. H.; Sodt, A.; Steele, R. P.; Rassolov, V. A.; Maslen, P. E.; Korambath, P. P.; Adamson, R. D.; Austin, B.; Baker, J.; Byrd, E. F. C.; Dachsel, H.; Doerksen, R. J.; Dreuw, A.; Dunietz, B. D.; Dutoi, A. D.; Furlani, T. R.; Gwaltney, S. R.; Heyden, A.; Hirata, S.; Hsu, C.-P.; Kedziora, G.; Khalliulin, R. Z.; Klunzinger, P.; Lee, A. M.; Lee, M. S.; Liang, W.; Lotan, I.; Nair, N.; Peters, B.; Proynov, E. I.; Pieniazek, P. A.; Rhee, Y. M.; Ritchie, J.; Rosta, E.; Sherrill, C. D.; Simmonett, A. C.; Subotnik, J. E.; Woodcock, H. L., III; Zhang, W.; Bell, A. T.; Chakraborty, A. K.; Chipman, D. M.; Keil, F. J.; Warshel, A.; Hehre, W. J.; Schaefer, H. F., III; Kong, J.; Krylov, A. I.; Gill, P. M. W.; Head-Gordon, M. Advances in Methods and Algorithms in a Modern Quantum Chemistry Program Package. *Phys. Chem. Chem. Phys.* **2006**, *8*, 3172−3191.
(53) Szabo, A.; Ostlund, N. S. *Modern Quantum Chemistry: Introduction to Advanced Electronic Structure Theory*; McGraw-Hill, 1989.
(54) Jensen, F. *Introduction to Computational Chemistry*; sons, J. W. and, Ed.; John Wiley and sons, 2007.
(55) Calvo-Castro, J.; Kennedy, A. R.; McHugh, C. J. Role of H-Optimization in the Computed Intermolecular Interactions and Charge-Transfer Integrals in Diketopyrrolopyrroles. *J. Phys. Chem. A* **2019**, *123*, 3185−3193.
(56) Boys, S. F.; Bernardi, F. The Calculation of Small Molecular Interactions by the Differences of Separate Total Energies. Some Procedures with Reduced Errors. *Mol. Phys.* **2002**, *100*, 65−73.
(57) Calvo-Castro, J.; McHugh, C. J.; McLean, A. J. Torsional Angle Dependence and Switching of Inner Sphere Reorganisation Energies for Electron and Hole Transfer Processes Involving Phenyl Substituted Diketopyrrolopyrroles; a Density Functional Study. *Dyes Pigm.* **2015**, *113*, 609−617.
(58) Simmler, L. D.; Rickli, A.; Schramm, Y.; Hoener, M. C.; Liechti, M. E. Pharmacological Profiles of Aminoindanes, Piperazines, and Pipradrol Derivatives. *Biochem. Pharmacol.* **2014**, *88*, 237−244.

https://dx.doi.org/10.1021/acsomega.0c01370
ACS Omega XXXX, XXX, XXX−XXX